

Unstable Solar, Interplanetary, and Geomagnetic Fields During Solar Cycles 23 and 24

Preeti Pandey^{1*}, Pramod Kumar Pandey²

¹Research Scholar, Department of Physics, Pandit S. N. Shukla University, Shahdol, India

²Professor, Department of Physics, Pandit S. N. Shukla University, Shahdol, India

Abstract: Short-term and long-term shifts in cosmic ray intensity (CRI) are caused by the sun's outputs and fluctuations. The observed correlation between solar activity and sunspots, solar radio radiation at 10.7 centimeters, coronal mass ejections (CM Es), and solar flares is strong. Furthermore, coronal mass ejections are linked to several plasma and field disturbances in the interplanetary medium. The data used to create this visualization comes from neutron monitors in Moscow, Oulu, and Keil, and it is based on monthly mean count rate variations in cosmic ray intensity (CRI) observed by the Omni web data center for solar-interplanetary data activities between 1996 and 2017. During the lowest of solar cycle 23 and the ascending part of solar cycle 24, we measured a record high value of cosmic ray intensity with low values of solar interplanetary activity parameters.

Keywords: HMF, Cosmic Rays, CRI, solar Cycle 23 and 24.

1. Introduction

The GCRs outside the heliosphere are thought to be isotropic in both time and space. The heliospheric magnetic field (HMF) embedded in the solar wind interacts with GCRs as they enter the heliosphere, causing random motion, diffuse inward motion, gyrating around the IMF, scattering at irregularities in the field, gradient and curvature drifts, etc. Cosmic rays were therefore modified in the heliosphere as a result of the combined impact of all these activities. As a result, we see notable fluctuations in their strength or energy spectrum inside the heliosphere at both a global and temporal scale. The complicated climatic circumstances present between the Earth and Sun area have a significant impact on the research of the FD phenomena. FDs often have rigidity-dependent magnitudes, with minimal amplitude near the equator and largest at the pole. Due to inward diffusion along the interplanetary magnetic field and outward convection along the solar wind, we also see secular fluctuation in NMs counts. Anisotropy in cosmic rays' results from the equilibrium between diffusion and convection. Several NM sites at about the same latitude and various longitudes must be averaged in order to overcome daily variance. In 2011, The solar energetic particle flow often has an impact on cosmic rays as well. Concurrent measurements of space plasma, magnetic field, and global NMs aid in understanding the physics behind cosmic-ray modulation. The primary initiators of FDs are corotating interaction regions (CIRs) and interplanetary coronal mass ejections (ICMEs).

The solar magnetic field, which is transported outward by solar wind plasma, dominates the heliosphere, a region of space. Due to random movements, galactic cosmic rays penetrate the heliosphere, diffuse inward toward the sun, whirl around the interplanetary magnetic field (IMF), and disperse at field abnormalities. The combined impact of these processes will modulate the distribution of cosmic rays in the heliosphere (Forman et al 1975). They will also undergo gradient and curvature drifts (Isenberg & Jokipii 1979), are converted back toward the boundary by solar wind, and lose energy via adiabatic cooling.

2. Data Analysis

In solar cycles 23 and 24 (as well as in the maxima of these cycles and the lowest between them), it has been compared between recurring (related with high-speed streams from coronal holes) and sporadic (produced by interplanetary coronal mass ejections, or ICMEs) Forbush declines (FDs). We were able to use statistical approaches because the Forbush Effects and Interplanetary Disturbances database, which was constructed and maintained in IZMIRAN, supplied a significant number of events (about 1700 solitary FDs, 350 recurrent FDs, and 207 random FDs picked with high confidence). The findings showed that recurrent FDs predominated at the lowest between cycles whereas sporadic FDs predominated in the maxima of cycles. Particularly at the maxima of the cycles, FD characteristics (magnitude, decline rate, and anisotropy) are higher for random events than for recurring ones. For sporadic events, FD magnitude is larger at peaks than minima, and it hardly varies for recurring ones. In general, recurring events have higher solar wind velocities than sporadic ones; recurrent FDs have higher velocities in the minimums while sporadic FDs have higher velocities in the maximum. In the maxima, the magnetic field is stronger for random FDs than recurrent ones, and in the lowest, it is about equal for both kinds of events. The magnetic field of ICMEs is less now than it was in the last solar cycle. Both kinds of events had shorter primary phases of FDs in their maxima; in cycle 23's maximum, sporadic FDs developed noticeably more quickly than recurring ones. From 2008 through 2021, six significant Forbush drop (FD) episodes of solar cycles 24 and 25 were detected by five neutron

*Corresponding author: preetipandey227@gmail.com

monitoring sites located in Rome, Moscow, Fort Smith, Oulu, and Thule. On November 3, 2021, July 15, 2017, September 6, 2017, June 21, 2015, September 11, 2014, and March 7, 2012, these occurrences were noted. In an attempt to understand the potential reasons that contributed to the occurrence of the big FD, an inquiry has been conducted. Numerous severe solar and planetary occurrences were examined throughout the inquiry. Sunspot counts, the disturbance storm time (Dst) index, and the Ap index are a few of them. We also looked at the solar wind's speed, density, temperature, and Bz component of the interplanetary magnetic field (IMF). The Dst index has a dramatic decline during the event time that is comparable to the Forbush reduction. Prior to the start of the FD, there were more sunspots, which suggests that this phenomenon may be related to the occurrence of solar flares, which further affect the variance in cosmic rays. It was discovered that there was a considerable southerly Bz drop, a rapid rise in solar wind temperature and speed, and that no major FD showed any evidence of density impact.

Interplanetary coronal mass ejections (ICMEs) and stream/corotating interaction regions (SIRs/CIRs) that originate in the Sun and are transmitted as a low-energy plasma disturbance through the interplanetary magnetic field (IMF) are the main causes of geomagnetic storms and Forbush decreases (FD) on Earth. In this article, we investigate the changes in the solar wind parameters (solar wind velocity, plasma density, and IMF-Bz component) and the Earth's disturbance storm-time index (Dst) in relation to cosmic ray flux measurements from 8 neutron monitor stations dispersed over Canada, Russia, Finland, and Greenland, during 3 intense geomagnetic storms that occurred during the 24th solar cycle (March 16–18, 2015, June 21–23, 2015, and September 7–9, 2017). The conventional two-step FD with a peak period of around 2.1 h is clearly evolving, according to the wavelet analysis of cosmic ray intensity. The correlation-delay study reveals a very good correlation (0.9) between the indices of solar wind speed and Dst and the relative count rate variations in cosmic ray intensity. The time-delay responses to the solar wind speed are consistent across all instances (4 h), however there are significant differences in the Dst index across the storms. As a result, we advise against utilizing the Dst index to forecast Forbush reductions. In the end, we parameterize the Forbush reductions in terms of the solar wind using the obtained delay times, and we arrive at a prediction model with an R2 parameter that is around 0.8. Additionally, we see a potential relationship between solar wind proton density and the strength of Forbush drops under situations of identical solar wind speed. Our findings support the usefulness of solar wind characteristics in forecasting Forbush declines in cosmic ray output.

Measurements from space and the ground are necessary for the study of the consequences of space weather, particularly more especially Forbush drops in cosmic ray intensity. Precursory indications, or pre-increases and/or pre-declines shown in cosmic-ray behavior, are often seen in conjunction with Forbush decreases and geomagnetic storms. These fluctuations in cosmic-ray intensity don't start just when the shock arrives; they start up to 24 hours in advance. This

research looked for antecedents in a collection of significant Forbush drops with amplitude 4%. The occurrences were divided into three groups based on the helio-longitude of the solar source: western (21circ leq) helio-longitude 60; eastern (60circ leq) helio-longitude (leq -21circ); and central (-20circ leq) helio-longitude (leq 20circ). The chosen events range from 1967 to 2017. The "Global Survey Method" and the "Ring of Stations" methods, respectively, were the foundations for the analysis of the Forbush reductions and the charting of the asymptotic longitudinal cosmic-ray distribution diagrams. Additionally employed were information on solar flares, solar wind speed, interplanetary magnetic field, and geomagnetic indices (Kp and Dst). The findings reveal that a sizable percentage of incidents had identifiable predecessors.

Magnetic storms are a result of extraterrestrial disturbances that hit the earth's shielding magnetic field. The Dst index is often used to gauge the intensity of geomagnetic storms. Significant storms in geomagnetic activity have been shown to be caused by interplanetary manifestations of coronal mass ejections (ICMEs). Its primary phase is distinguished by a significant reduction in Dst during geomagnetic storms. Sudden reduction in cosmic ray intensity (CRI) is a hallmark of the Forbush decline. Due to their shared point of origin, forbush reduction and geomagnetic storms are thought to be closely associated. Increased magnetic fields in solar ejecta and interplanetary shocks that protect the Earth from galactic cosmic rays (GCRs) are what lead to forbush dips (FDs) in neutron monitor (NM) counting rates. Those ejecta's solar origins may be seen in coronagraphs as coronal mass ejections (CMEs), but their motion through interplanetary space close to or beyond the Earth has not before been witnessed. In this article, we looked at the extraterrestrial variables related to powerful geomagnetic storms and Forbush deaths. The research has made use of hourly measurements of the geomagnetic activity, cosmic ray intensity (CRI), and solar wind plasma.

3. Cycle 23 Versus the Past History

We first overlaid the falling stages of all cycles by matching them on a tie point corresponding to the downward crossover at $Ri = 25$ in the smoothed monthly sunspot number using the sunspot index record of the previous 24 cycles, for which the data coverage is the most extensive. The recent 23–24 minimum was not an exceptional example, according to this superimposed–epoch figure. Additionally, it demonstrates how the four groups of cycle rise phases—fast, moderate, late, and weak rises—are grouped together after a minimum. The Dalton minimum's cycles 4, 5, and 6 belong to the latter category. In contrast to the preceding minimum, which was an example of the quickest increases, the 23–24 minimum fits the group of late rises. The most recent example of the steadily ascending cycles is the 14–15 minimum, which dates back to 1913.

We also want to point out that, if prior activity patterns repeat themselves, a low cycle 24 with a maximum Ri of 90 should follow this somewhat lengthy minimum, according to this comparison of all cycle minima. The previous low was also distinguished by a series of protracted sunspot-free intervals and a high aggregate number of spotless days (817 days). Figure

shows a graph of the total number of clear days for each activity minimum during the last 250 years. Despite the fact that the peak of spotless days for cycles 23–24 is rather high, it is surpassed by four additional minima and approaches intermediate levels recorded for the majority of previous solar cycles, with the exception of recent cycles 19–22. In contrast, spanning more than 200 years of systematic sunspot monitoring, the consistent run of low spotless days counts of cycles 19–22 creates a unique occurrence in this case.

As a result, whereas cycle 23 seems to be a return to the usual moderate activity regime, the recent string of strong cycles really represents a Grand Maximum, a rare enhanced-activity anomaly at secular timeframes as a result, given that they mostly rely on data from the last 50 years, contemporary measurements and proxies, as well as their interpretation, may be subject to a Grand Maximum bias. So, it may be dangerous and inaccurate to simply extrapolate current data and models into the distant past.

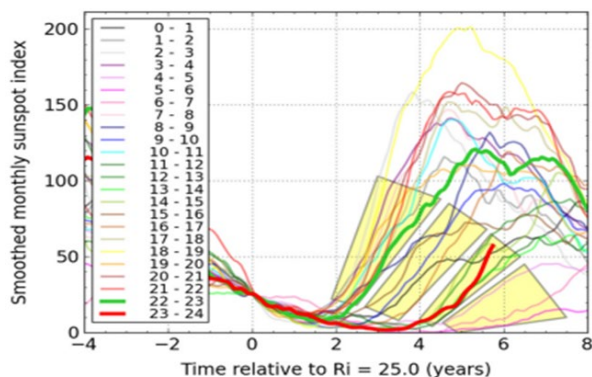


Fig. 1. Superposed-epoch plot of the Ri index obtained by aligning all solar cycles 0–23 on their Ri = 25 crossing point in the final decaying phase of the cycle

4. Solar Cycle 24

The most recent solar cycle, cycle 24, is the 24th since systematic records of solar sunspot activity started in 1755. It lasted from December 2008 to December 2019, with a minimum smoothed sunspot number of 2.2. Up to the start of 2010, activity was sparse. It peaked in April 2014, with a sunspot number of 81.8 after 23 months of smoothing. This maximum value was far lower than those of earlier recent solar cycles, reaching levels last seen between cycles 12 and 15 (1878–1923).

It is important to look at the forecasts made for Cycle 24, the cycle we are presently at the conclusion of, before thinking about what could occur in the future. Many solar physicists felt they had a thorough knowledge of what causes such cycles when Cycle 23 came to an end in the middle of the first decade of the twenty-first century while studying the Sun to witness the first stirrings of Cycle 24. Despite this, Cycle 24 projections were wildly inconsistent. It was even predicted that this cycle would be the strongest ever. Overall, it was the weakest cycle in the previous 100 years. The US National Oceanic and Atmospheric Administration (NOAA) first forecast it would begin in March 2007, but when it didn't, they changed their

estimate to March 2008 and then had to adjust it once again. Only Svalgaard came up with an accurate forecast. Small sunspots at high latitude that develop 12 to 20 months before to the beginning of a new cycle are the earliest sign of a new cycle. They didn't start to show up until the beginning of 2010, which made the sunspot minimum between Cycles 23 and 24 exceptionally protracted.

'This is the lowest we've ever seen,' a scientist once said about the Sun. In 2009, Marc Hairston of the University of Texas said, "We thought we'd be out of it by now, but we're not." And more than simply sunspots are raising alarm. The so-called solar wind, or streams of particles the Sun spews forth, is also at its lowest point in recorded history. The magnetic axis of the Sun is also slanted in a unique way. According to NASA solar scientist David Hathaway, "This is the quietest Sun we've seen in almost a century." With 82 sunspots at its peak in April 2014, Solar Cycle 24 achieved its peak. The Northern Hemisphere of the Sun dominated the sunspot cycle, reaching its peak more than two years before the Southern Hemisphere. Some astronomers were surprised by Cycle 24's rather lackluster performance. There existed a little business that attempted to forecast the future using statistics from sunspot data, but it had not been entirely effective. It has become clear in the last twenty years that more study should be done on the physics of the solar cycle, particularly in light of Cycle 24's statistics. Predictions will only be more accurate when physics is taken into consideration in addition to sunspot data.

5. Characteristics of Sars in Solar Cycle 24

To explain the vector field characteristics of SARs and FARs in cycles 22 and 23, we utilized the vector magnetograms of the Solar Magnetic Field Telescope at Huairou Solar Observing Station and four magnetic field parameters. The four variables were the net magnetic flux, total photo spheric free magnetic energy density, length of the magnetic neutral line with steep horizontal magnetic gradient (300 G Mm), region with severe magnetic shear (shear angle 80), and total photo spheric free magnetic energy density. We developed a composite vector field index, or I_{com} , based on the statistical findings of the four SAR and FAR parameters. It was discovered that $I_{com} 1.0$ was used for the bulk of SARs. In this Chapter, we calculate the aforementioned four parameters and the I_{com} of SARs in Solar Cycle 24 using the vector magnetograms of the Helio seismic and Magnetic Imager onboard the Solar Dynamics Observatory which have a spatial resolution of 1 and a time resolution of 12 min.

The Space weather HMI Active Region Patch (SHARP) data which had been translated from the picture plane into the heliographic coordinate system by the HMI team, provided the vector magnetograms. We only use magnetograms that are close to the central meridian in order to increase the accuracy of our findings. We chose a lower area threshold of FAR for the present cycle since there aren't any FARs in accordance with the definition of FAR in Chapter II until August 31, 2015. We designate to an AR as a FAR if it produced no flares higher than the M1.0 class and covered an area bigger than 800 h. Two FARs are investigated and compared to the SARs.

Table 1
The vector magnetic field parameters of SARs in solar cycle 24

	NOAA	$ \Phi_{net} $ (10^{22} Mx)	E_{free} (10^{24} erg cm^{-1})	L_{NL} (Mm)	$A_{\Psi}(\Psi \geq 80^\circ)$ (Mm^2)	I_{com}
SARs	11429	0.18	0.68	53.14	154.75	1.02
	11520	0.22	0.73	16.67	404.96	1.35
	11944	1.21	0.30	25.33	144.33	1.04
	11967	1.51	1.43	87.65	316.47	2.32
	12192	1.26	0.57	35.07	103.22	1.10
FARs	12108	0.09	0.04	6.45	12.59	0.13
	12109	0.46	0.05	3.93	24.33	0.26

Table 1 contains the values for the aforementioned four parameters as well as I_{com} 's five SAR and two FAR values for Cycle 24. The correlation between I_{com} and the soft X-ray flare index of 19 SARs and 10 FARs in cycles 22–24 is shown in Fig. The two SAR parameters seem to have a strong linear association, with a linear correlation coefficient of 0.69. The confidence level is examined using a t-test, and the association has a confidence level greater than 99%. With an $I_{com} > 1.0$, all of the SARs (red circle) in Cycle 24 have the traits of the SARs (red plus) in Cycles 22 and 23.

But none of the FARs' I_{com} s (blue circle) are higher than 1.0. All of the SARs and FARs in the three cycles would be easy to differentiate if the I_{com} threshold was lowered to 0.9 (see the green dashed-dotted line). The I_{flare} and the I_{com} of SARs in Cycle 24 are all substantially lower when compared to SARs in Cycles 22 and 23. It was evidently CME-poor; out of tens of big flares, only an M4.0 flare was connected to a CME during Cycle 24's two SARs, which had the highest sunspot area since December 1990.

6. Variability in Occurrence of CMEs and Resulted Mass Loss Rate During Solar Cycles 23 and 24

The most immediate, important, and often used measure of solar activity is the solar activity cycle, which has an average duration of 11 years.

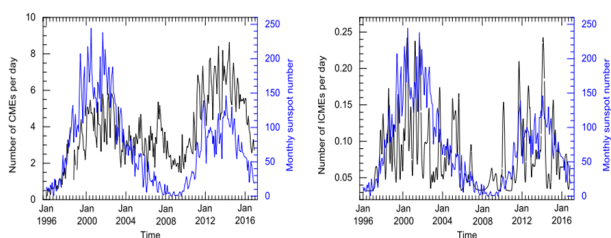


Fig. 2. Left-hand panel: the variation of rate of CMEs (on the left Y-axis in black) and monthly sunspot number (on the right Y-axis in blue) with time (on X-axis) during solar cycles 23 to 24 is shown. Right-hand panel: Similar to the left-hand panel, but for ICMEs.

Are how many sunspots there are on the solar photosphere. The trustworthy record of sunspots spans more than a century. According to Wolf's system of numbers, the period from the years 1755 to 1766 is known as the A1' solar cycle. solar cycle 23 is projected to last from August 1996 to December 2008, peaking around 2002. Additionally, it experienced a protracted solar minimum that was very quiet. According to Pesnell the solar cycle 24 started in December 2008, reached its peak in the middle of 2014, and is now in its decreasing phase. In terms of

disruptions in the convection zone, solar surface, and heliosphere, solar cycle 24 is reported to be weaker than its previous solar cycle.

A. Occurrence Rate of CME and ICME with Sunspot Number

From the Coordinated Data Analysis Workshops (CDAW) CME catalogue ([https://cdaw.gsfc.nasa.gov/CME list/](https://cdaw.gsfc.nasa.gov/CME_list/); Yashiro et al. 2004), we were able to collect the information on the CMEs that were seen during cycles 23 and 24. The catalog is a list of CMEs that were captured by the Solar and Heliospheric Observatory (SOHO) mission's Large Angle and Spectrometric Coronagraph (LASCO; Brueckner et al. 1995). Images from the C2 and/or C3 coronagraphs are used to identify CMEs because the LASCO initially carried three coronagraphs with overlapping fields of view (C1: 1.1-3 R, C2: 2-6 R, and C3: 3.7-32 R), of which the C1 could not survive after the temporary loss of the SOHO spacecraft in 1998.

We restrict our study for solar cycle 24 to the years 2009 through 2016 since the CME observations for the full year of 2017 and beyond are not recorded in the archive. The SIDC website where the sunspot data are found. We include all CME events reported in the catalogue, independent of their morphological and kinematic properties, even if they are rated as "very poor" events, in order to determine the occurrence rates of CMEs. The CDAW collection covers 28315 CMEs seen with SOHO/LASCO from January 1996 to December 2016. We determined the average number of CMEs every day by first counting the CMEs in a calendar month.

7. Conclusion

The measured magnitudes of magnetic irregularities offer some regular structure in the interplanetary field necessary for propagation of powerful solar flare particles to provide magnitude of initial intensity lowered and seen. The conditions for the formation of a massive FD are optimal when a huge solar flare erupts on the Sun's surface. Cosmic ray intensity measurements at neutron monitor energies show a Forbush reduction 24-72 hours after a major solar flare. After a delay of many hours, geomagnetic storms (SSC) began abruptly. The shock front of the accelerated solar wind is heralded by the SSC. The early weakening of Earth's exposure to cosmic rays is caused by this shock front, or magnetic field discontinuity. There is a positive association between the long-term profile of annual mean high speed solar wind streams and the annual mean fluctuation of the geomagnetic disturbance index (A_p) ($r = 0.76$). It is possible to formulate a three-dimensional balancing equation for this kind of tangential discontinuity (Lockwood, 1971).

References

- [1] Melkumyan, Anaid & Melkumyan, Anaid & Belov, Anatoliy & Belov, Anatoliy & Abunina, Maria & Abunina, Maria & Abunin, Artem & Abunin, Artem & Eroshenko, Evgeniya & Eroshenko, Evgeniya & Oleneva, Victoria & Oleneva, Viktoria & Yanke, Viktor & Yanke, Viktor. (2019). Recurrent and sporadic Forbush decreases during solar cycles 23–24. Solar-Terrestrial Physics. 5. 28-34.
- [2] Shalaby, S. & Darwish, A. & Ayman, Aly & Hanfi, M. & Ambrosino, Fabrizio & Alqahtani, Mohammed & Elshoukrofy, Abeer. (2023).

- Analysis of a significant Forbush depression of solar cycles 24 and 25 (2008–2021). *The European Physical Journal Plus*. 138.
- [3] Baral, Rabin & Adhikari, Binod & Calabria, Andres & Shah, Munawar & Mishra, Roshan & Silwal, Ashok & Bohara, Sudarshan & Manandhar, Roshna. (2022). Spectral Features of Forbush Decreases during Geomagnetic Storms. *Journal of Atmospheric and Solar-Terrestrial Physics*. 242. 105981.
- [4] Papailiou, M. & Abunina, Maria & Mavromichalaki, H. & Belov, A. & Abunin, Artem & Eroshenko, E. & Yanke, Victor. (2021). Precursory Signs of Large Forbush Decreases. *Solar Physics*. 296.
- [5] Singh, Sham & Singh, Kalpana & Pandey, Ashish & Tiwari, Chinta & Mishra, V & Mishra, A. (2018). Cosmic-Ray Modulation in relation to Solar and Heliospheric Parameters.
- [6] Dhurve, Lt. Arvind & Saxena, Anil & Ghuratia, Rani. (2022). Variations of Cosmic ray intensity in relation to Sunspot Number and Solar Wind Parameters over the period 1996-2019. *International Journal of Scientific Research in Science and Technology*. 9. 418-423.
- [7] Bhoj, Chandrasekhar & Prasad, Lalan & Pokharia, Meena & Mathpal, (2019). Study of the cosmic ray intensity in relation to geomagnetic storms and solar interplanetary parameters for solar cycles 21 and 23. *Journal of Astrophysics and Astronomy*. 40.
- [8] Agarwal, Rekha & Shra, Rajesh & Yadav, M & Pandey, Surendra. (2011). Cosmic Rays and Space Weather Prediction. *Proceedings of the 32nd International Cosmic Ray Conference, ICRC 2011*. 11.
- [9] Bazilevskaya, Galina & Cliver, Edward & Kovaltsov, Gennady & Ling, Alan & Shea, M. & Smart, D. & Usoskin, I. (2014). Solar Cycle in the Heliosphere and Cosmic Rays. *Space Science Reviews*. 186. 409-435.
- [10] Bhattacharya, R. & Roy, Misha & Barman, Paavana & Mukherjee, C. (2013). A Journey Through Researches on Cosmic Rays. 5. 784-795.
- [11] Maghrabi, Abdulrahman & Kudela, K. & Aldosari, A. & Almutairi, Munif & Altilasi, M. (2021). Short-term periodicities in the downward longwave radiation and their associations with cosmic ray and solar interplanetary data. *Advances in Space Research*. 67.
- [12] Goyal, Sanjay & Chaurasiya, Deepak & Shrivastava, P. (2023). Study of solar parameter and interplanetary medium with geomagnetic parameter on the solar cycle 24 Citation.
- [13] Oh, Suyeon & Yi, Y., (2017). Variations in Solar Parameters and Cosmic Rays with Solar Magnetic Polarity. *The Astrophysical Journal*. 840. 14.
- [14] Dergachev, Valentin & Vasiliev, Sergey & Raspopov, O.M. & Jungner, Hogne. (2012). Impact of the geomagnetic field and solar radiation on climate change. *Geomagnetism and Aeronomy*. 52.
- [15] Bhargawa, Asheesh & Singh, Ashok. (2020). Ascendancy of Solar Variability on Terrestrial Climate: A Review. *Journal of Basic & Applied Sciences*. 16. 105-130.